LARGE-SCALE HORIZONTAL FLOWS FROM SOUP OBSERVATIONS OF SOLAR GRANULATION

L.J. November (NSO/SP), G.W. Simon (AFGL/SP), T.D. Tarbell,
A.M. Title, and S.H. Ferguson (LPARL)

ABSTRACT

Using high-resolution time-sequence photographs of solar granulation from the SOUP experiment on Spacelab 2, we have observed large-scale horizontal flows in the solar surface. Our measurement method is based upon a local spatial cross correlation analysis. The horizontal motions have amplitudes in the range 300 to 1000 m/s. Radial outflow of granulation from a sunspot penumbra into surrounding photosphere is a striking new discovery. We see both the supergranulation pattern and cellular structures having the scale of mesogranulation. The vertical flows that are inferred by continuity of mass from these observed horizontal flows have larger upflow amplitudes in cell centers than downflow amplitudes at cell boundaries.

1. Introduction

Since the Doppler effect measures line-of-sight velocities it cannot be used to determine horizontal motions at disk center. The only way to observe such flows is through proper motion studies using solar features as tracers. Granules are the obvious choice as tracers of photospheric flows, but because of their small size, coupled with the blurring and geometric distortion due to atmospheric turbulence, they have proven to be difficult to use in ground-based observations (Simon 1967). During its 10 minute lifetime, a typical granule might move only a few hundred kilometers, about one-third of an arcsec, which is much less than the size of the random fluctuations caused by atmospheric seeing, even under the best conditions.

Now, however, with the high-quality distortion-free movie sequences from SOUP, we can measure granulation proper motions with high accuracy. The SOUP image quality was so good (pointing jitter was about 0.003 arcsec, or 2 km on the sun) that we can measure flow speeds to an accuracy of 15 - 20 m/s rms. This is much less than errors in the flow measurements due to random motions and evolution of individual granules and the residual effects of the large-scale five-minute oscillations. Analysis of these various "solar noise" contributors indicates an overall error of about 80 m/s per independent spatial sample in the results to be discussed below. This is far smaller than the 300 - 1000 m/s signals which we report.

Some of the preliminary results have already been reported (Title et.al. 1986, November et.al. 1986b).

2. Technique

Proper motion is determined from these data by computing the displacement that maximizes the cross-correlation between two image fields separated by a time Δt. In our analysis we have used values of Δt from 10 to 60 s. The images are first filtered to remove some photographic grain noise and any large- scale intensity gradients so that the remaining signal is mainly the solar granulation. Then the cross-correlation function is computed at each "locale" on the images. The locale around each image point is defined as the product of the intensity field and a gaussian window centered on that point. The gaussian window used in this analysis had a full width at half maximum (FWHM) of 4.2 arcsec. The vector displacement and transverse flow velocity of the features within the window during the interval Δt are then found by locating the cross-correlation maximum. The window is moved from pixel to pixel over the entire image to give the vector displacement at every pixel locale. This computational method is described by November (1986a). The 4.2 arcsec size of the gaussian was found to be a reasonable compromise between sensitivity and resolution in the final map of transverse flow velocities. We have developed a similar algorithm at Lockheed that uses the minimum of a squared residual function. The agreement in displacements measured by the two techniques is excellent.

Figure 1 is an example of a vector displacement map formed by averaging 160 original vector maps spanning 1600s of time. The window size is plotted in the lower left of each figure; this represents the actual spatial resolution of the displacement measurements. Note that we considerably oversample this resolution in the analysis and display vectors formed from overlapping granulation fields.

We have calibrated this technique by cross-correlating a digitized photographic image with itself after applying a known spatial shift in the microdensitometer digitizing stage. The precision depends very sensitively upon the method used for interpolation in the cross-correlation. With the data sampled at or exceeding the diffraction limit of the telescope, a 2–D quadratic interpolation to

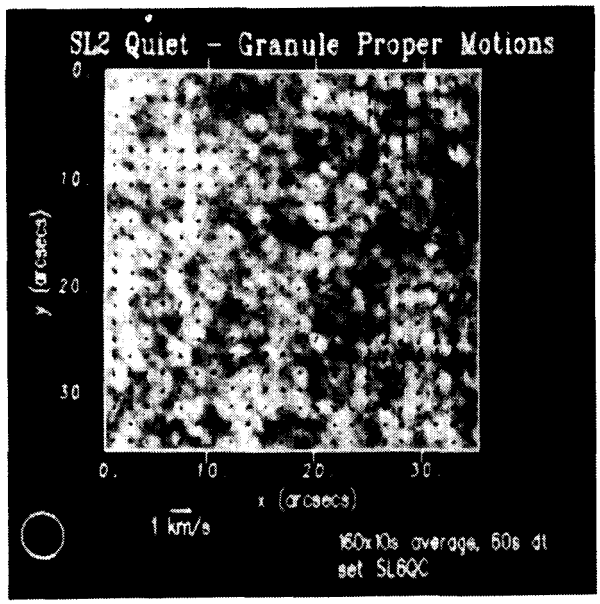

Figure 1. Average proper motion vector map – quiet region. The proper motion at each spatial locale has been defined by spatial cross-correlation analysis within a sliding gaussian window. The granulation is shown with superposed vectors having lengths proportional to the amplitude of the local flows. The scale of the vectors is given by the arrow shown below these figures. The gaussian window size of 4.2 arcsecs FWHM is indicated by the size of the circle in the lower left. This vector map is formed from the average of 160 original vector maps and spans 1600s in time.

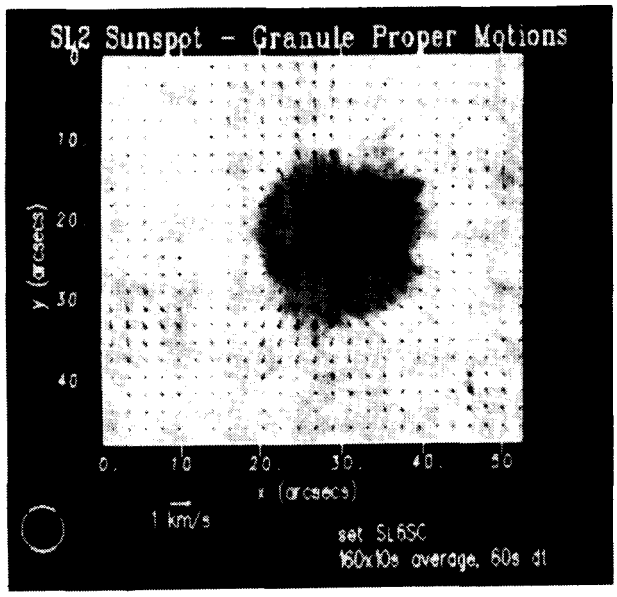

Figure 2. Average proper motion vector map – sunspot region. A large isolated spot was photographed by SOUP, and shows radial outflow from the penumbra and nearby photosphere. No vectors are shown in the umbra of the sunspot as there was inadequate signal there for the cross-correlation.

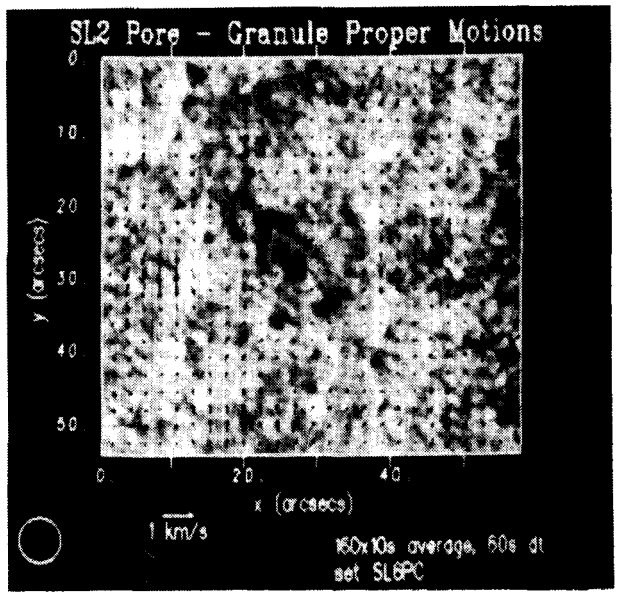

Figure 3. Average proper motion vector map – pore region. This is a region containing numerous pores. Notice that the amplitude of the flows is considerably reduced in the vicinity of the pores. Away from the pores cellular flows characteristic of those seen in the quiet sun image are again apparent.

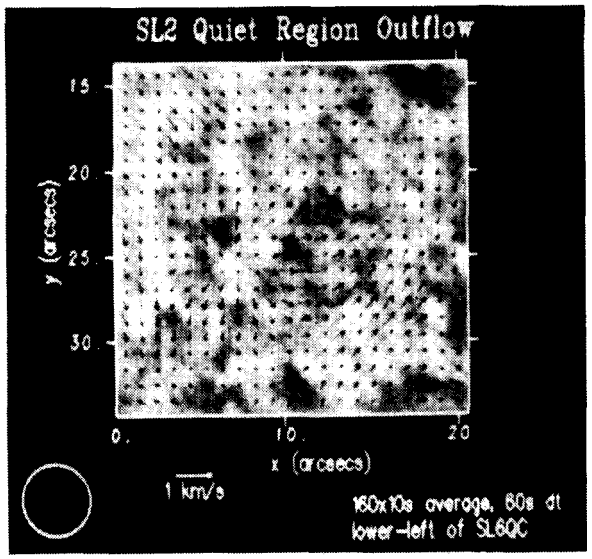

Figure 4. A magnified portion of the quiet proper-motion map from Figure 1 is magnified and more vectors are displayed. This demonstrates the cellular nature that is characteristic of the large-scale proper-motion flows.

the cross-correlation gives a measurement of the image shift having a bias error of less than 3 percent for displacements in the range 0.005 pixel (0.6 km on the sun) to 0.5 pixel.

The error in the measurement is estimated by examining the evolution of the vector displacement in time. We compute a time-averaged vector displacement map as in Figure 1; the fluctuations about this average give an upper estimate of the noise in the measurement. The Fourier power spectrum of this temporal variation shows two components: a low-frequency feature and a smaller high-frequency white-noise tail. The tail reflects the statistical uncertainty in the measured displacement and is probably due principally to photographic granularity noise. It contributes an rms error of 20 m/s, or 0.01 pixel, to the 160 frame average of vector displacements. The low-frequency component has maximum power at about 200s period and contributes an rms error of 80 m/s to the average. The level of this "solar noise" may vary from quiet sun to plage or sunspot regions.

3. Analysis

Three specific portions of the 166x250 arcsec, 160 frame, 27 minute data set have been analyzed: a region of quiet sun, an isolated sunspot, and a pore region. This data set was obtained between 19:10 and 19:38 UT on 5 August 1985, in the vicinity of NOAA active region 4682. Single frames of these image fields are shown with their overlying average vector proper motions, respectively, in Figures 1, 2, and 3. Each of these images was produced by digitizing positive copies of the original films. Let us look at these figures in some detail.

In the quiet sun photograph (Figure 1) we identify two regions of larger horizontal outflow emanating from centers at (34,17) and (8,25) (that is to say, the coordinates of the outflow center (34,17) are at x=34 arcsec and y=17 arcsec in the figure). We have magnified the area centered at (8,25) and show it in Figure 4. Here we see also a nearby linear sink region around (15,22). Flows which emanate from single points and then flow toward and along a line are fairly characteristic of quiet- region velocity patterns. However, note the nice exception showing convergence to a point at (25,34) in Figure 1. This small region is magnified in Figure 5. The scale of many of the cellular features is typically 10 arcsec; we associate this with mesogranulation (November, et.al. 1981).

The region around (34,17) in Figure 1 is shown enlarged in Figure 6. This feature has the typical supergranule scale of about 30 - 40 arcsec (Simon and Leighton 1964). The outflow in this example appears to show abrupt changes in flow direction partitioned along radial lines approximately 45 degrees apart: note the lines of flow from (34,17) to (25,10), from (34,17) to (25,17), and from (34,17) to (28,24). We can understand this structure by analyzing the divergence of the horizontal flow $\mathbf{u} = (u,v)$, $\nabla\cdot\mathbf{u} = \partial u/\partial x + \partial v/\partial y$. The divergence is shown in Figure 7 as contours superposed on the quiet granulation field from Figure 1. Here we identify the outflow at (34,17) as the large positive divergence that reaches an amplitude of $5.5\cdot10^{-4}$ s^{-1}. This outflow is surrounded by smaller cells. Apparently the superposition of the flows from the smaller cells creates the impression of the radial velocity structure.

One large sunspot was observed in the area photographed by SOUP. Figure 2 shows this region with superposed flow vectors. Radial outflow extends from the edge of the sunspot penumbra into surrounding photosphere with amplitude 300 - 700 m/s. This annulus or "collar" around the penumbra has a width of about five arcsec. This outflow is reduced adjacent to two small sectors of penumbra, one of which is poorly-formed and intermediate in brightness between normal penumbra and photosphere. We show in Figure 8 the sunspot region with superposed contours of flow divergence. Away from the sunspot we find cellular inflows and outflows similar to those seen in the quiet region of Figure 1.

Figure 3 shows a region containing numerous pores with superposed flow vectors. The granule proper motions are much reduced in the pore region, but away from the pores we again find cellular inflows and outflows as in the quiet sun. The lack of flow in the pore region is illustrated by the small amplitude of the divergence signal over the pores shown in Figure 9. The region in the immediate vicinity of the pores is magnified in Figure 10, and here the reduced magnitude of flow vectors can be clearly seen. The flow velocities in the pore region are about 100 m/s, about the size of the "solar noise" in our measurements, and thus difficult to observe.

4. Discussion

In the divergence maps of the cellular quiet sun flows, we find that the places of positive divergence characteristically have larger amplitudes than the places of negative divergence even though in its definition the average divergence over the area of the image is set to zero. Compare, for example, the extremes of divergence in Figure 1 at region (8,25) with $5.5\cdot10^{-4}$ s^{-1} and the region at (24,31) with divergence $-4.5\cdot10^{-4}$ s^{-1}. We quantify the difference between upflow and downflow regions by plotting a histogram of the divergence. It extends to larger amplitudes for the positive divergences. The mean of the positive divergence is $1.29\cdot10^{-4}$ s^{-1} and the mean of the negative divergence is $-1.17\cdot10^{-4}$ s^{-1}; thus the sinks occupy more area than the sources.

The sinks and sources are associated with downflows and upflows through the mass con-

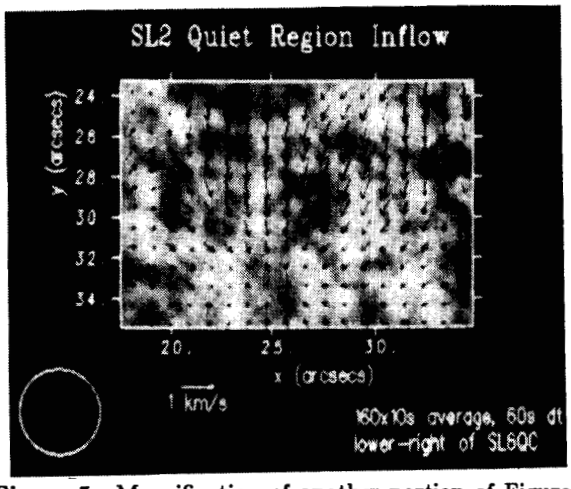

Figure 5. Magnification of another portion of Figure 1 to show a sink point. More typically, however, sources are isolated points, while sinks lie along lines of convergence.

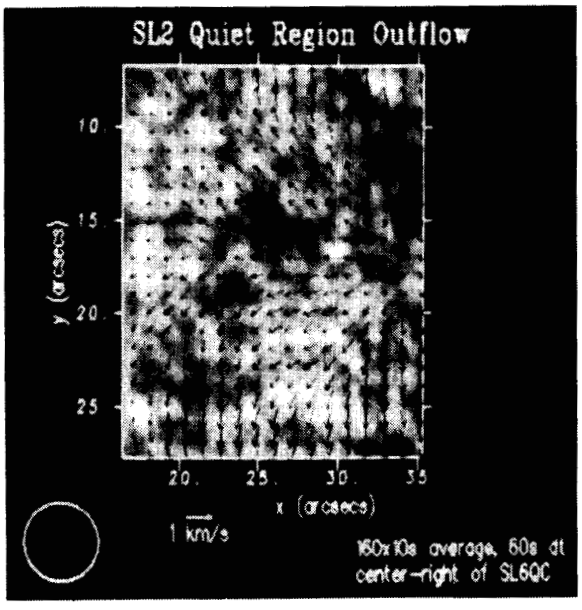

Figure 6. Magnification of a third part of Figure 1 showing a large supergranular cell.

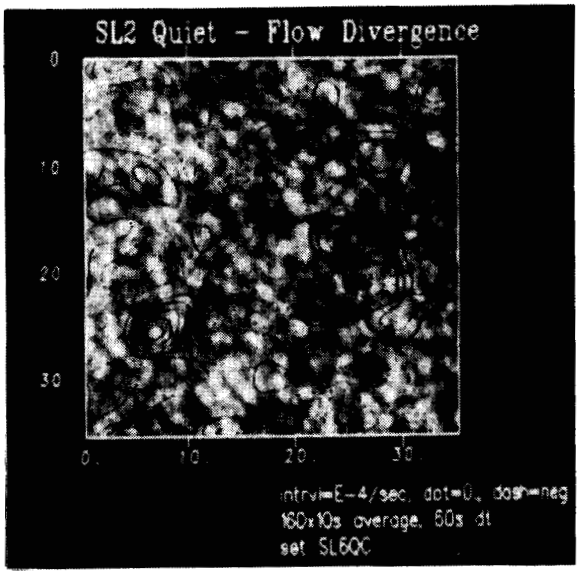

Figure 7. Divergence of quiet-region flows. The contours show the amplitude of the local divergence of the horizontal flows from Figure 1. The contour interval is $1{\cdot}10^{-4}$ s^{-1}. Point source regions are those with positive divergence (solid contours), while the linear sink regions have negative divergence (dashed contours). The zero contour is dotted.

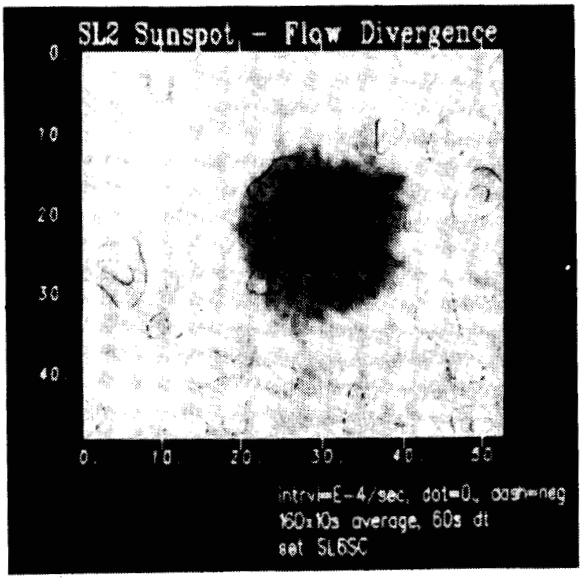

Figure 8. Divergence of sunspot-region flows shown in Figure 2.

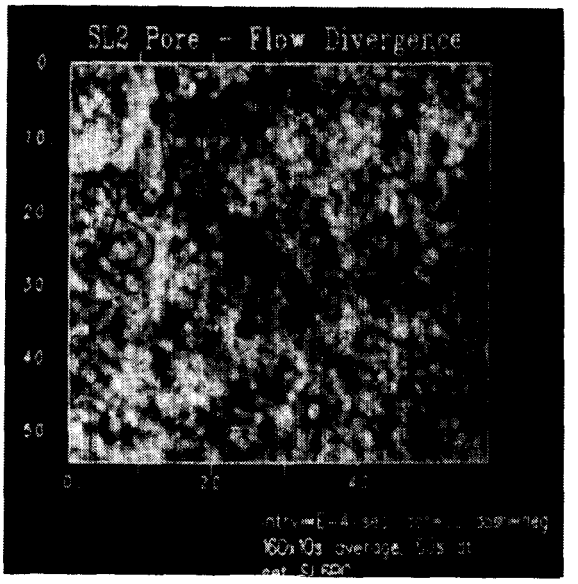

Figure 9. Divergence of pore-region flows from Figure 3.

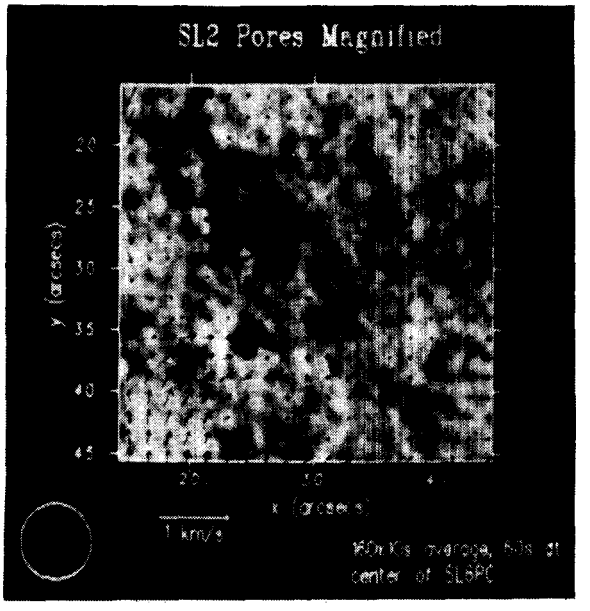

Figure 10. Pore region magnified. This shows the vectors in the immediate vicinity of the pores from Figure 3. The amplitude of the flow is considerably reduced here relative to the quiet sun flows.

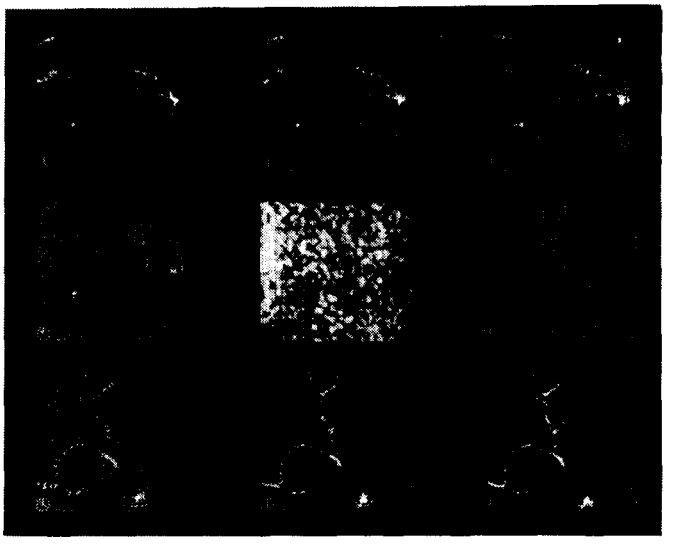

Figure 11. Propagation of long-lived tracers. "Corks" embedded in the flow field of Figure 1 trace out the flow pattern from their emergence in regions of positive divergence until they congregate in sinks and network regions where the divergence is negative. The nine frames proceed from -8 to $+8$ hours with the actual observation time (hour 0) shown as a superposed uniform grid of corks and granulation intensity in the center frame.

tinuity equation: $\partial(\rho w)/\partial z = -\nabla\cdot(\rho \mathbf{u})$, where w is the vertical and $\mathbf{u}$ the vector horizontal velocity. We rewrite this as: $(w/\rho)\cdot(\partial\rho/\partial z) + \partial w/\partial z = -\nabla\cdot\mathbf{u}$. The horizontal density fluctuations at any level must be small because the mean density is defined by the local pressure which is mainly hydrostatic, and by the temperature which is approximately fixed at a given depth. Replacing $1/\rho\cdot\partial p/\partial z$ with $1/h_\rho$, and $\partial w/\partial z$ with w/h_w, where h_ρ and h_w are the density and velocity scale heights, respectively, we obtain $w(\,1/h_\rho + 1/h_w\,) = -\nabla\cdot\mathbf{u}$. Letting $(1/h_\rho + 1/h_w) = 1/h_m$ where h_m is the mass flux scale height, then assuming $h_w << h_\rho$ (Schmidt, et.al. 1985), and using a value of h_ρ=200 km for the subphotosphere, $h_m \simeq$ 200 km and we obtain w=26m/s as the average of the sources and w=−23m/s as the average of the sinks. These values, smaller than the noise in earlier Doppler measurements, explain why it has been so difficult to detect vertical velocities in supergranulation.

The sense of our flow fields is like that of typical Benard cells that have greater central upflows than downflows at the boundaries (Chandrasekhar 1961). Further, the small amplitudes which we infer are in general agreement with Doppler measurements of the vertical flows in the supergranulation. Simon and Leighton (1964) were unable to detect vertical motions at disk center although their sensitivity was better than 100 m/s. More sensitive Doppler measurements (Frazier 1970, Worden and Simon 1976, Giovanelli 1980, November, et.al. 1982, Küveler 1983) give vertical amplitudes similar to those we infer here. Our proper motion measurements are, however, in qualitative disagreement with the Doppler observations which showed larger amplitude downflows than upflows. Thus they probably reflect another effect. The difference might be explained as a systematic error in the Doppler signal caused by a possible contrast effect in granulation over magnetic elements (Giovanelli 1980). More likely, the Doppler observation could result from a superposition of photospheric flows that are dominated by magnetic rather than convective processes in the network boundaries (Giovanelli 1980, Gebbie, et.al. 1981).

The large-scale flow fields, both as observed visually from the movies, and quantitatively from the calculated vector displacements, have the proper size and appearance of super- and mesogranular convection flows. Therefore we would expect these flows, at subsurface levels in the sun, to move magnetic fields to the cell boundaries, and form the loci of the photospheric and chromospheric networks. The SOUP white-light movies indeed give us the definite impression that lanes of brighter-than average granules occur at these places (converging sinks and line flows) where the divergence is negative, i.e. at the cell boundaries. This bright photospheric network always seems to surround the upwellings, or boiling centers, which mark the darker-appearing super- and mesogranule centers. Unfortunately we have not yet been able to locate from ground-based data any good quality magnetogram or chromospheric spectroheliogram coincident with these SOUP data. These are needed to make a definitive comparison with our flow fields. SOUP data from earlier and later orbits are currently being reduced. Some of these do coincide with National Solar Observatory images of sufficiently high quality to make useful comparisons. We hope to analyze these data in the next few months.

Implicit in our analysis is the assumption that the granules float, like corks, on the supergranular flows, and thus can serve as tracers to define the larger structures. Suppose, then, that we start with a uniform distribution of granule "corks" superposed on and subject to the pattern of arrows which define our average flow fields. As time evolves, the corks move, and as they reach the next pixel point, they are subjected to the slightly different flow field corresponding to that location. We have made a movie of such cork flows in which we extrapolate our measured velocities forward and backward in time assuming that they do not change over the 36 hour length of the movie. It is interesting to note that the corks form into a network pattern in two to three hours; some of the corks, as expected, congregate at the few sink holes in our images. If we run such a cork movie in reverse, the corks quickly concentrate in the upwellings which form the meso- and supergranule centers. We illustrate the cork motions in Figure 11 where we show the movie frames from times −8, −6, −4, −2, 0, 2, 4, 6, and 8 hours relative to the actual time of observation for the quiet sun image of Figure 1. While these cork movies give only an artificial picture of the development of large-scale flows, they do agree well with our intuition. Fortunately there exist, in all, about 16 hours of SOUP data so that it will be possible to make an authentic study of the evolution of these flows.

References

Chandrasekhar, S., *Hydrodynamic and Hydromagnetic Stability*, Oxford University Press, 1961.

Frazier, E.N., "Multi-Channel Magnetograph Observations II. Supergranulation", *Solar Phys.* ***14***, 89-111, 1970.

Gebbie, K.B., Hill, F., Toomre, J., November, L.J., Simon, G.W., Gurman, J.B., Shine, R.A., Woodgate, B.E., Athay, R.G., Bruner, E.C., Rehse, R.A., Tandberg-Hanssen, E.A., "Steady Flows in the Solar Transition Region Observed with SMM", *Astrophys. J.* ***251***, L115-L118, 1981.

Giovanelli, R., "The Supergranule Velocity Field", *Solar Phys.* ***67***, 1980.

Küveler, G., "Velocity Fields of Individual Supergranules", *Solar Phys.* ***88***, 13-29, 1983.

November, L.J., Toomre, J., Gebbie, K.B., Simon, G.W., "The Detection of Mesogranulation on the Sun", *Astrophys. J.* **245**, L123-L126, 1981.

November, L.J., Toomre, J., Gebbie, K.B., Simon, G.W., "Vertical Flows of Supergranular and Mesogranular Scale Observed on the Sun with OSO−8", *Astrophys. J.* **258**, 846-859, 1982.

November, L.J. "Measurement of Geometric Distortion in a Turbulent Atmosphere", *Applied Optics* **25**, 392-397, 1986a.

November, L.J., Simon, G.W., Tarbell, T.D., Title, A.M., and the SOUP Team, "Precise Proper Motion Measurement of the Solar Granulation", *B.A.A.S.*, June 1986b.

Schmidt, H.U., Simon, G.W., Weiss, N.O., "Buoyant Magnetic Flux Tubes II. Three-Dimensional Behavior in Granules and Supergranules", *Astron. Astrophys.* **148**, 191-206, 1985.

Simon, G.W., "Observations of Horizontal Motions in Solar Granulation: Their Relation to Supergranulation", *Zeitschrift für Astrophysik* **65**, 345-363, 1967.

Simon, G.W., Leighton, R.B., "Velocity Fields in the Solar Atmosphere III. Large-Scale Motions, the Chromospheric Network, and Magnetic Fields", *Astrophys. J.* **140**, 1120-1147, 1964.

Title, A.M., Tarbell, T.D., Simon, G.W., and the SOUP Team, "White-Light Movies of the Solar Photosphere from the SOUP Instrument on Spacelab 2", *Proceedings of* COSPAR 26th Plenary Meeting, Toulouse, France, June 1986.

Worden, S.P., Simon, G.W.," A Study of Supergranulation using a Diode Array Magnetograph", *Solar Phys.* **46**, 73-91, 1976.